공학석사 학위논문

Fabrication of Micropatterned ZnO Semiconductor Films via Chemical Imprinting

화학적 임프린팅을 이용한 마이크로패턴의 산화아연 반도체 박막 형성에 관한 연구

2013년 2월

서울대학교 대학원

융합과학부 나노융합전공

성 기 은

Fabrication of Micropatterned ZnO Semiconductor Films via Chemical Imprinting

지도교수 김 연 상

이 논문을 공학석사 학위논문으로 제출함

2013년 2월

서울대학교 대학원

융합과학부 나노융합전공

성 기 은

성기은의 석사 학위논문을 인준함

2013년 2월

위 원 장 박 원 철 (인)

부위원장 김 연 상 (인)

위 원 송 윤 규 (인)

Abstract

Fabrication of Micropatterned ZnO Semiconductor Films via Chemical Imprinting

Kieun Seong

Program in Nano science and Technology

The Graduate School

Seoul National University

Herein, we demonstrated a new patterning method via chemical imprinting with an ammonia-soaked PDMS stamp on the ZnO semiconductor films. The diffused ammonia liquid or gas from the PDMS stamp with fine structures selectively transformed the ZnO films to a water-soluble form (as $[Zn(NH_3)_{4-n}(OH)_n]^{2-n}$) at the contact surfaces, and these selectively transformed aqueous

salt patterns were dissolved in water. Thus, the array of ZnO micro-patterns were easily fabricated and successfully applied to the active layers of TFTs. In addition, we fabricated the micro-patterns on Li doped ZnO semiconductor films, which have high carrier mobility and low temperature sintering at 300 °C. The present study demonstrates the representative micro-patterned Li doped ZnO TFTs with the field effect mobility of 4.2 $cm^2 \cdot V^{-1} \cdot s^{-1}$, on/off current ratio of 8.3 x 10^7 and low gate leakage current using this chemical imprinting. This patterning method has a good potential for advanced patterning process toward solution-processed ZnO TFTs with high performance; it can be applied to continuous processes at ambient conditions, such as the roll to roll process, and does not require any cumbersome steps.

Keyword : imprint lithography, soft lithography, solution-processed zinc oxide (ZnO), thin film transistors (TFTs), selective chemical etching

Student Number : 2011-22754

Contents

List of table, schemes and figures

1. Introduction

1.1 Oxide Thin Film Transistors

Thin film transistors (TFTs) based on metal oxide semiconductors, such as indium (In), gallium (Ga) and zinc (Zn) oxides compound (IGZO), have garnered increasing interests as switching or driving components for advanced displays, such as active matrix liquid crystal displays (AM-LCDs) and active matrix organic light emitting diode (AM-OLED) displays.[1-4] This is because they possess a high field effect mobility, large on/off current ratio, and stable current reliability.[5] In addition, the metal oxide semiconductors have high optical transparency in visible light region due to their wide band gap (Eg > 3.3 eV); therefore, metal oxide semiconductors present the opportunity to develop transparent electronic devices.[6,7] Various vacuum techniques such as pulsed laser deposition (PLD),[8] radio frequency (RF) sputtering,[9] metal organic chemical vapor deposition (MOCVD)[10]and atomic layer deposition (ALD),[11] all of which

ensure outstanding electrical performance, have been applied to deposit the metal oxides as semiconducting layers in TFTs. However, despite their remarkable electrical features, the batch-type vacuum deposition processes continue to have the fundamental problem that the vacuum deposition instruments require high level investments. Thus, solution processibility under ambient conditions has been focused on as an advanced device fabrication process that is capable of achieving low-cost, large-area, and mass manufacturing. The studies on solution process for high performance ZnO TFTs has continued; otherwise, the patterning for solution-processed ZnO semiconductors remains problematic.

1.2 Thin Film Transistor Structure and Operation

Figure 1 shows a description of the basic TFT structure including a-Si, poly-Si, and ZnO based semiconductors.[12] The channel layer is produce with source and drain electrodes that are able of efficient carrier injection into source and extraction from drain the channel region. The gate electrode is separated from the channel, source, and drain by a thin gate dielectric film. The dimensions of this structure are the channel width (W) and length (L), and the gate dielectric thickness (t_{gd}); the active channel region are composed of the rectangular area between the source and drain electrodes.

Figure 2 illustrates the TFT operation along the voltage and charge polarities for an n-type device which has the channel current of electrons as carriers. A voltage applied to the gate electrode modulates the charge density in the channel through the capacitance of the gate dielectric to channel voltage differential is accompanied by a corresponding gate to channel electric field, mediated by the formation of space charge layers of equal magnitude and opposite sign, located on the opposite sides of the

gate dielectric. The magnitude of the induced charge density is proportional to the applied gate voltage; in the channel, this variation in charge density produces a corresponding variation in source to drain conductance. For an n-type device, as depicted in Figure 2, a positive gate voltage draws additional electrons into the channel, while a negative gate voltage reduces the channel electron density. This modulation of source to drain conductance exhibit as drain current (I_D) via an applied gate voltage comprises the fundamental component of field-effect transistor (FET) functionality.

TFT operation is typically quantified in the form of drain current (I_D) as a function of gate-to-source voltage (V_{GS}) and drain-to-source voltage (V_{DS}). With the appropriate selection of simplifying assumptions, the widely recognized ideal Metal-Oxide Semiconductor Field Effect Transistor (MOSFET) standard model equation is obtained.

$$I_D = \begin{cases} 0 & \cdots V_{GS} \le V_{T,} \\ \mu \ C_{ins}\frac{W}{L}[(V_{GS}-V_T)V_{DS}-\frac{V_{DS}^2}{2}] & \cdots V_{DS} \le V_{GS}-V_{T,} \\ \frac{1}{2}\mu C_{ins}\frac{W}{L}[V_{GS}-V_T]^2 & \cdots V_{DS} > V_{GS}-V_T \end{cases}$$

μ, C_{ins}, and V_T are the channel mobility, gate dielectric capacitance per unit area, and threshold voltage, respectively. While this expression may not provide quantitative agreement with devices that deviate substantially from one or more of the relevant model assumptions, it nonetheless comprises a useful qualitative basis for understanding the key elements of TFT operation.

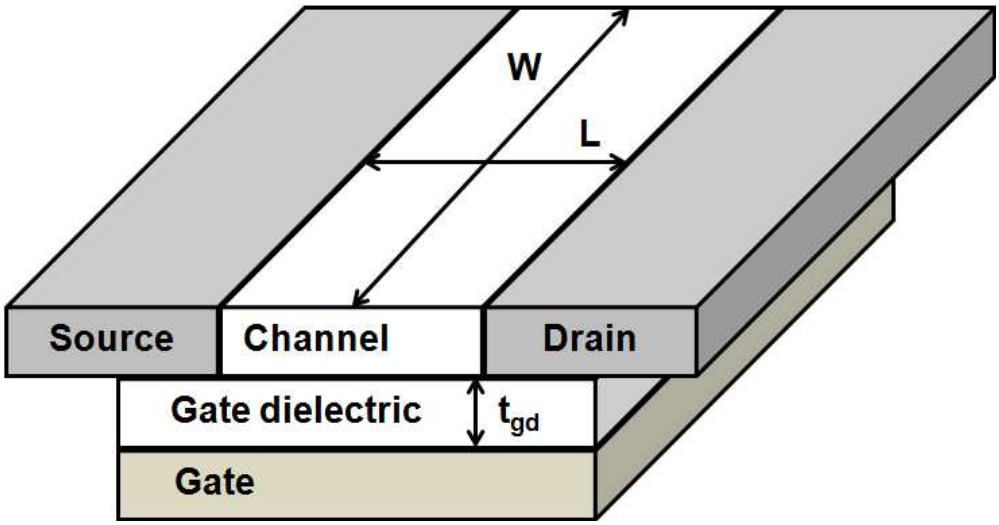

Figure 1. Simplified schematic depiction of the basis TFT structure.[12]

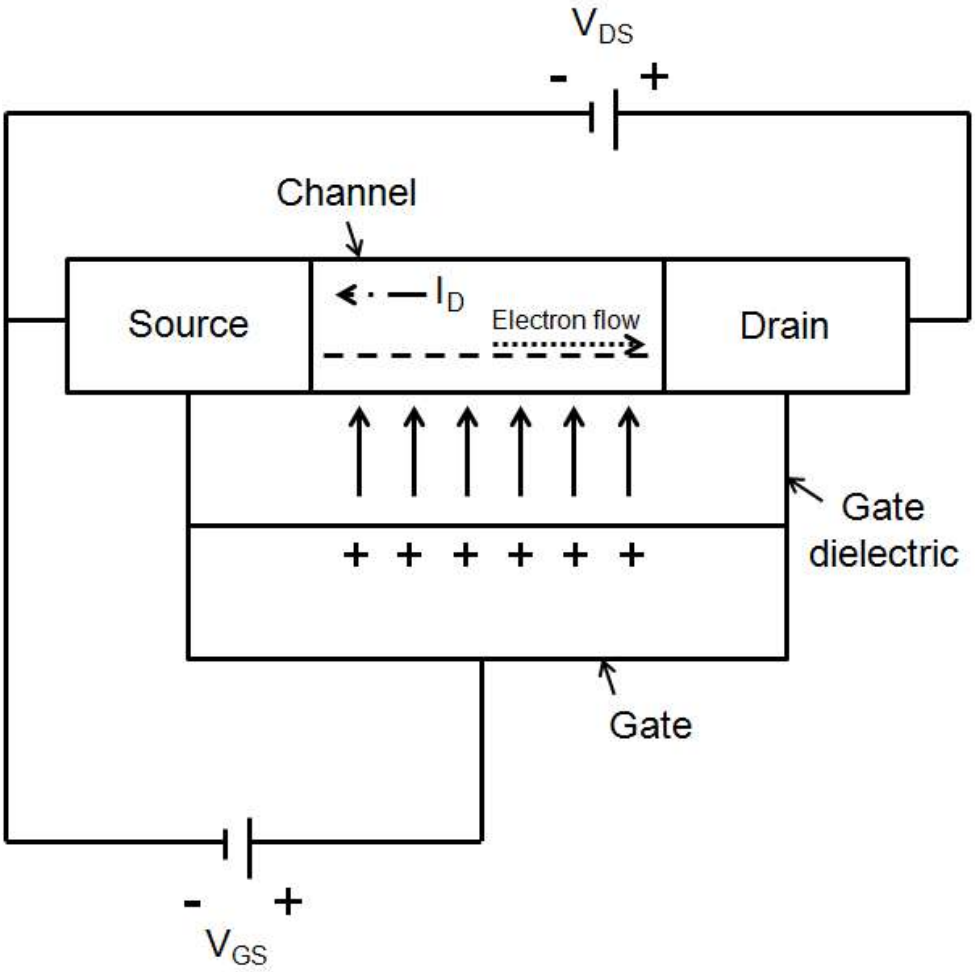

Figure 2. Schematic illustration of the central elements of TFT operation.[12]

1.3. Patterning Process

Patterning process is th key technological driving force for the overall microelectronics which is controlled by the rate of advances in micro-lithographic tools, methods, and materials.[13] Of a variety of electronics, we focused on the appropriate patterning process for TFTs. Patterning is an essential process for the TFT arrays, because it prevents the potential leakage current and cross-talks between the adjacent devices,[14] which cause problems such as low definition of display.[15] However, there are some challenges for the development of patterning techniques of solution-processed ZnO semiconductor films. In general, the ZnO semiconductors are easily damaged by the acid or the base solutions used for developing and stripping processes in photolithography due to their intrinsic amphoteric property.[16] In addition, in the stripping process, the residual photoresist materials cause the degradation of the interface between the active layer and the insulator because the solution-processed ZnO thin films have a porous structure.[17] Moreover, ZnO thin films are vulnerable to plasma treatment during a dry etching

process.[18] To overcome these limitations, an alternative patterning method is required for maximizing the potential of solution-processed ZnO TFTs.

Non-conventional lithography, such as inkjet printing and microcontact printing, has a good potential to fabricate the patterned ZnO semiconductor films. Inkjet printing as a direct patterning method with solution processibility shows good performance in the patterning process; however, this method is still subject to degradation of electron mobility in TFTs. This is because the inkjet printing with the ZnO precursor solutions easily induces the wavy, porous and non-uniform patterns in the drying step due to their uneven volatile properties.[19,20] Microcontact printing is another alternative method to fabricate the patterned ZnO semiconductor films. Rothwell et al. reported the microcontact printing method for ITO or IZO films with poly(dimethylsiloxane) (PDMS) stamp using self-assembled monolayers (SAMs) of alkanephosphonic acids and wet etching with the oxalic acid solution.[21] Through PDMS stamp, alkanephosphonic acids were printed selectively on ITO and IZO thin films and then etched in the aqueous oxalic acid solution. As

the selectively printed alkanephosphonic acid components reacted firmly with ITO or IZO thin films, they were good hydrophobic barriers to the aqueous etchant. In spite of good patterning, the researchers had significant problems with the application in fabricating TFTs. When an electrode evaporation was carried out on the patterned semiconductor films using SAMs (such as alkanephosphonic acids), it brought out an interface problem induced by the SAMs between the semiconductor films and electrodes, which caused the increase of resistance between the semiconductor films and electrodes and degraded the electron conduction and device performance. This is an intrinsic problem of conventional microcontact printing using SAMs.

1.4 Alkali Metal Doping

Recently, some remarkable results for the enhancement of the performance of solution processed ZnO TFTs have been introduced.[22,23] However, the requirement of In, which is a scarce but a strategically important material, is a potential difficulty.[24] In a previous research, a simple route to achieve high-performance and low-temperature, solution-processed ZnO TFTs by employing alkali metals doping with lithium (Li), sodium (Na), potassium (K) or rubidium (Rb) was introduced.[25] The alkali metal-doped TFTs not only showed excellent performance but also allowed the rare and expensive In or Ga element to be omitted. These TFTs, with high field effect mobility, over 7 $cm^2 \cdot V^{-1} \cdot s^{-1}$, have been successfully demonstrated using an ammine-hydroxo zinc complex and lithium complex precursor with low annealing temperature as maximum as 300 °C. This is because the alkali metal dopants, especially below 10 mol % Li dopants of ZnO were positioned at interstitial sites of ZnO matrix and tend to acting as the shallow donors and thus n-type doping.[26] Moreover, the presence of shallow donors

related to the intersititial Li and Na atoms on ZnO was demonstrated experimentally by a previous analysis based on electron paramagnetic resonance and electron nuclear double resonance experiments.[27]

2. Experimental Process

2.1 Materials, Fabrication and Characterization

Poly(dimethyl siloxane) (PDMS; Dow Corning), Zinc oxide(99.999%, Aldrich), Lithium hydroxide monohydrate (99.95%, Aldrich), Ammonia water (25.0~28.0 wt%; Daejung, Korea) and methanol(99.5%, Daejung, Korea) were used without purification.

The patterned ZnO thin films and the unpatterned ZnO thin films were characterized by a field emission scanning electron microscope (FE-SEM; S-4800: Hitachi), an atomic force microscope (AFM; XE100: PSIA) and a transmission electron microscope (TEM; JEM-2100F: JEOL) The current - voltage measurements were executed under ambient conditions by an Agilent 4155B semiconductor parameter analyzer.

2.2 Process of Chemical Imprinting

Scheme 1 illustrates schematically the patterning process for the ZnO semiconductor thin films. For preparation of the PDMS stamp, Si master was prepared through photolithography process on Si wafer. For the successful patterning of semiconductor films, we fabricated the semiconductor patterns (length of square: 500 μm, depth of patterns: 35 μm) on Si wafer via photolithography. PDMS base and curing agent (10:1) were poured out on Si master, which has positive relief in the petri-dish. For curing, the mixed materials were annealed at 80 °C for 4 hours, and then the PDMS stamp was peeled off from the Si master. To avoid uncured PDMS oligomers, the PDMS stamp was post-cured at 80 °C for an additional 12 hours. After that, the PDMS stamp with negative relief structure was obtained. The prepared stamp was soaked in the binary solvent composed of ammonia water and methanol (volume ratio, 5:5) for one hour. After one hour, the soaked stamp was blown with nitrogen gas to remove solvent on its surface.

For preparation of ZnO thin films as the semiconductor films,

0.001 mole of ZnO solution (ZnO powder 0.08139 g in 12 mL NH_4OH) was refrigerated for 5 hours to increase the solubility of ZnO.[28] The prepared solution was spin-coated (3000 rpm, 30 s) on Si wafer with a thermally grown SiO_2 layer (thickness ~ 200 nm). The ZnO thin films were cured at 300 °C for 1 hour. For fabrication high performance TFTs, 0.1 mL of LiOH solution (LiOH powder 0.2395 g in 10 mL de-ionized water) was added to the zinc oxide solution (ZnO powder 0.08139 g in 12 mL NH_4OH); this resulted in 10 % Li doped ZnO solution. The 10% Li doped ZnO precursor solution was spin-coated (3000 rpm, 30 s) on SiO_2 / Si wafer (SiO_2 thickness ~ 200 nm).

As the chemical imprinting process, the prepared stamp was contacted on ZnO thin films for 15 minutes to transform to the aqueous salt selectively in a refrigerator. After detaching the stamp from the ZnO thin films, the patterned ZnO thin films were washed with de-ionized water to dissolve the formed aqueous salt on the contact regions with PDMS stamp. To remove residual water and ammonia, the patterned ZnO thin films were post-annealed at 110 °C for 30 minutes to make only ZnO patterns. For fabricating high performance TFTs, chemical

imprinting was applied to Li doped ZnO thin films with the same process.

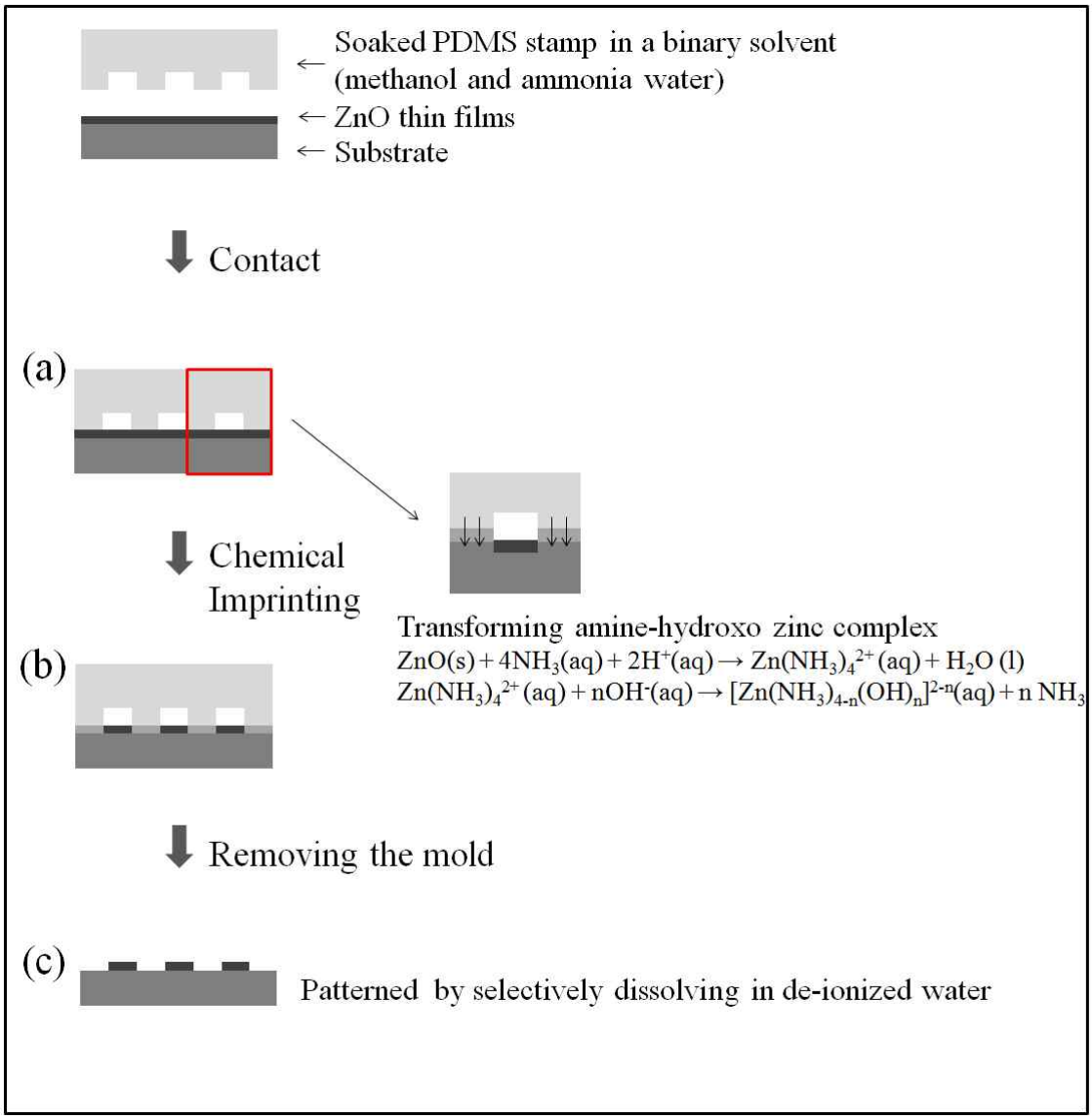

Scheme 1. Illustration of experimental schemes for the micro-patterned ZnO thin semiconductor films by chemical imprinting.

2.3 TFT Fabrication

Figure 3 shows the device structure of TFT including patterned ZnO thin films as semiconductors with bottom gate and top contact structure.

After the chemical imprinting, the TFTs were fabricated on patterned Li doped ZnO semiconductor films. The form of patterned Li doped ZnO semiconductor films were rectangular with a length of 500 μm. As source/drain electrodes, Aluminum (Al, 100 nm) was evaporated thermally on Li doped ZnO thin films. For comparison of the patterning effect, as unpatterned devices, the TFTs were fabricated on the spin-coated Li doped ZnO thin films with the same process as patterned devices. As a result, the patterned devices' width was 500 μm and length was 50 μm (W/L=10), while the unpatterned devices'width was 1000 μm and length was 50 μm (W/L=20).

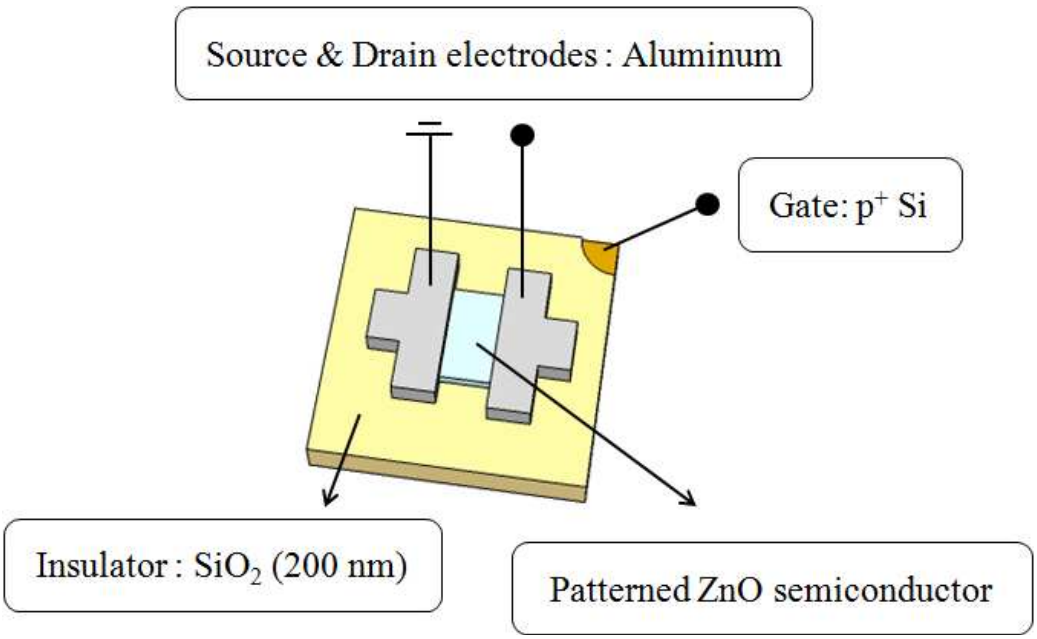

Figure 3. Device structure of patterned Li doped ZnO thin film transistor.

3. Result and Discussion

3.1 Solvent and PDMS Stamp

We used the binary solvent composed of methanol and ammonia water (the volume ratio, 5:5) to make the soaked PDMS stamp. For making soaked PDMS stamp, the methanol played a crucial role in the transfer the ammonia from the PDMS stamp to ZnO thin films. Ammonia water is based on water, the solution is difficult to soaking the PDMS stamp. As methanol retains the ammonia without any chemical reactions and does not swell the PDMS stamp,[29] this is a good carrier with reactants for chemical imprinting using PDMS stamp. After the one hour soaking in the binary solvent of methanol/ammonia water with PDMS stamp, for chemical imprinting, we used a conformal contact directly on ZnO films with PDMS stamp in the refrigerator (roughly between 2 °C and 5 °C) during 15 minutes. As ammonia water is likely to evaporate easily at room

temperature due to its low boiling point, the low temperature process confirmed the effective chemical imprinting process, preventing an excessive diffusion and evaporation of ammonia. In addition, ZnO is more likely to be the aqueous ZnO salt, $[Zn(NH_3)_{4-n}(OH)_n]^{2-n}$, at low temperature through the chemical reaction with ammonia,28 which could shorten the processing time in comparison to be processed at room temperature.

For adequate patterning process, the aspect ratio of PDMS stamp is considered. PDMS stamps have problems such as sagging and pairing due to low young's modulus.[30] We observed the sagging problem when the length of patterns were too long compared to the height of patterns. (length : 500 μm, height : 2 μm) For successful semiconductor patterning, we designed the PDMS stamp which have the micro-patterns as square form with 500 μm length and 35 μm height to avoid any problems induced by the aspect ratio of patterns.

Solvent	Swelling ratio
Methanol	1.02
Ammonia water	1.02

Table 1. Swelling ratio of the each solution composed of the binary solvent.[29]

3.2 Micro-patterned ZnO Thin Films

Patterned ZnO thin films were fabricated via chemical imprinting between binary solvent soaked PDMS stamp and ZnO thin films. To observe patterned ZnO thin films, scanning electron microscope (SEM) images were obtained. According to the patterns of PDMS stamp, reverse patterns were fabricated on ZnO thin films via chemical imprinting.

After chemical imprinting, the direct contact regions between PDMS stamp and ZnO films could be selectively dissolved in water because of the formation of aqueous ZnO salt, $[Zn(NH_3)_{4-n}(OH)_n]^{2-n}$, induced by ammonia water that flew out from the contact region of the PDMS stamp. The reaction mechanism of the ZnO films and the ammonia is shown in equations from (1) to (3).[25]

$$NH_3 + H_2O(l) \leftrightarrow NH_4^+(aq) + OH^-(aq),\ NH_4^+(aq) \leftrightarrow NH_3(aq) + H^+(aq) \cdots\cdots (1)$$

$$ZnO(s) + 4NH_3(aq) + 2H^+(aq) \rightarrow Zn(NH_3)_4^{2+}(aq) + H_2O(l) \cdots\cdots\cdots\cdots (2)$$

$$Zn(NH_3)_4^{2+} + nOH^-(aq) \rightarrow [Zn(NH_3)_{4-n}(OH)_n]^{2-n}(aq) + nNH_3 \cdots\cdots\cdots (3)$$

After contact for 15 minutes, the chemically imprinted ZnO films were washed by de-ionized water and then cleaned by nitrogen blowing. For the removal of residual de-ionized water, the micro-patterned ZnO films were placed on a hot plate at 110 °C for 30 minutes. Figure 4 and 5 confirmed the neat fabrication of micro-patterned ZnO films in chemical imprinting by SEM images and energy dispersive x-ray spectroscopy (EDS).

Figure 6 shows clearly the various micro-patterned ZnO films fabricated by chemical imprinting such as dots patterns (radius = 170 μm) and the line and space patterns (period = 20 μm). These scanning electron microscope (SEM) images indicate clearly that ammonia water reacted with ZnO thin films on the only contact regions between the PDMS stamp and ZnO thin films.

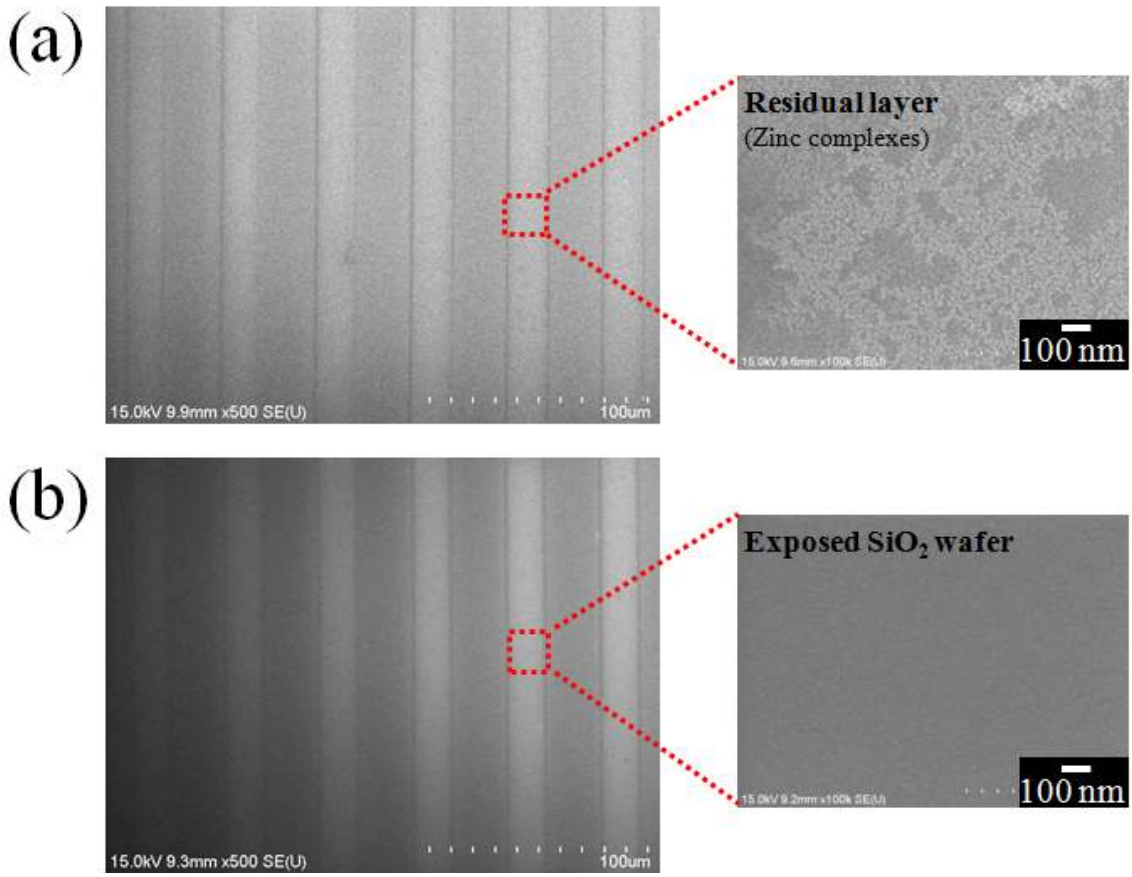

Figure 4. (a) ~ (b) SEM images of micro-patterned ZnO thin films. (a) the micro-patterned ZnO films after chemical imprinting. The SEM images showed the aqueous ammonia-ZnO salt forms on the region of chemical imprinting. (b) after rinsing with de-ionized water, no residual was shown in SEM image.

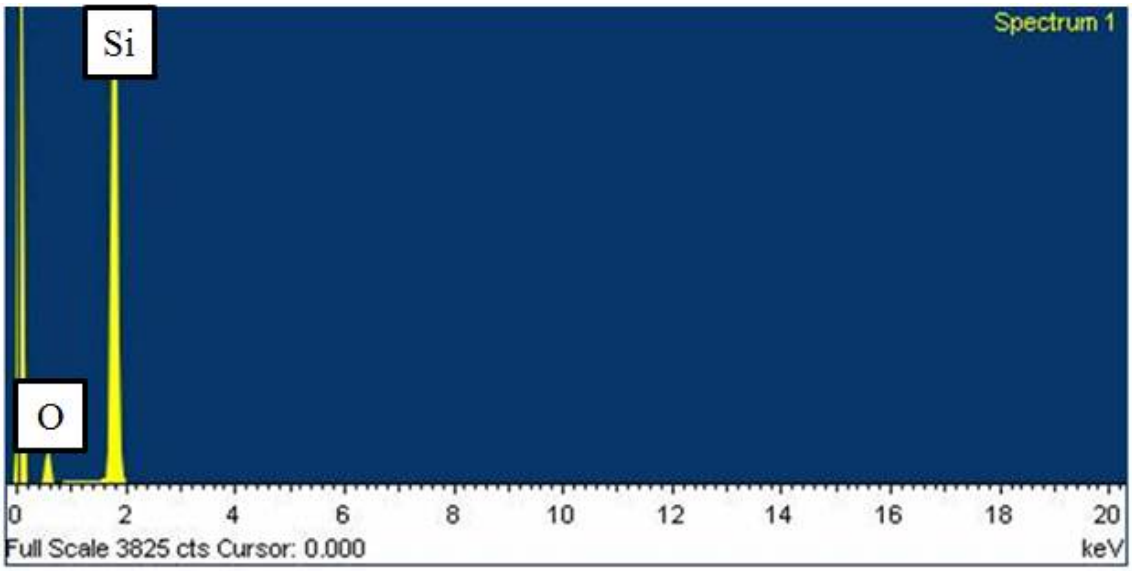

Figure 5. The EDS data of selectively exposed SiO_2 wafer indicated no residual layer of ZnO films.

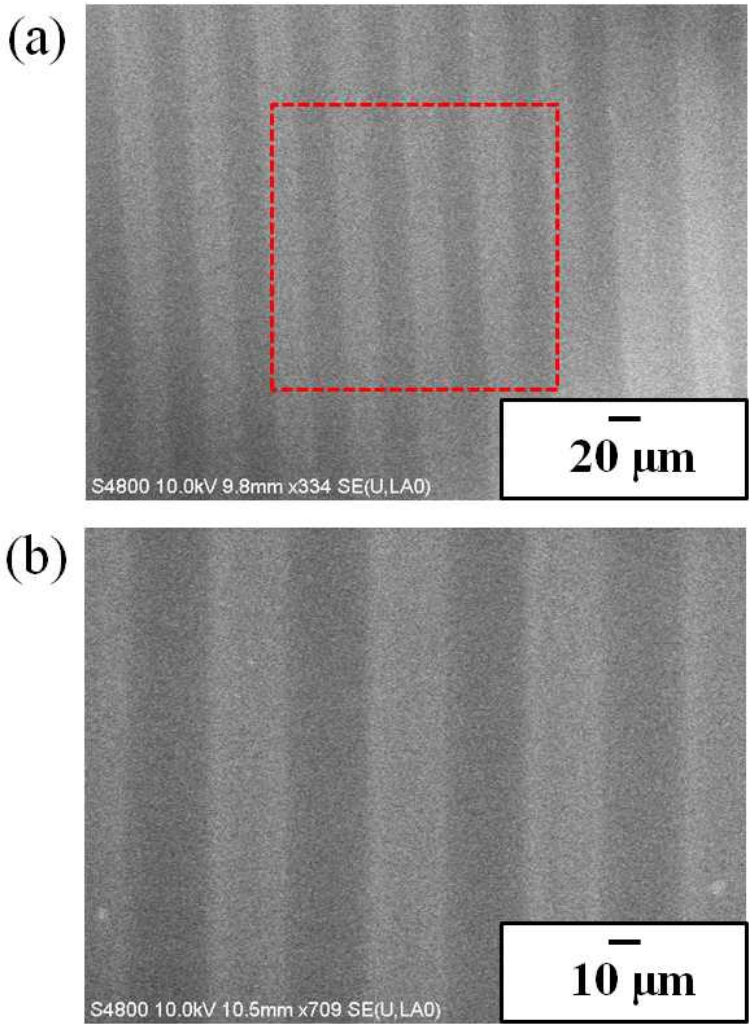

Figure 6. SEM images of line and space patterns of ZnO thin films with 20 μm repeating.

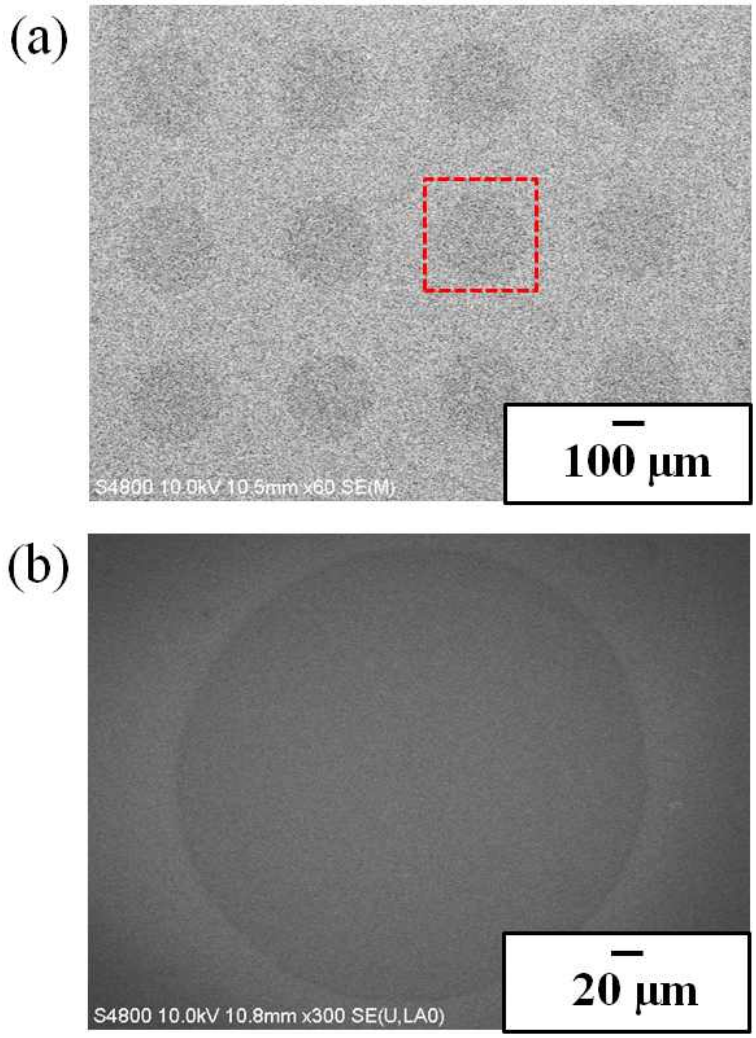

Figure 7. SEM images of dot patterns which have the radius 170 μm patterns of ZnO thin films.

3.3 Study on the Effect of Chemical Imprinting

To investigate the effect of chemical imprinting for solution processed ZnO thin films, the cross-sectional images of the micro-patterned ZnO thin films and pristine ZnO thin films were compared by transmittance electron microscope (TEM). Before measurement of the TEM images, the thin poly (methyl methacrylate) layer was spin-coated on ZnO thin films to avoid penetration of platinum (Pt). Thickness of patterned ZnO thin films was measured as ~ 7 nm , which is the same as the thickness of the pristine ZnO thin films in figure 8. In addition, the TEM images indicated that the crystal lattices of ZnO were not disturbed by chemical imprinting.

To characterize the change of surface morphology and crystalline phase of ZnO, an atomic force microscope (AFM) was performed, as shown in figure 9. There was no significant change of morphology, which means that the patterning process didn't degrade the ZnO films.

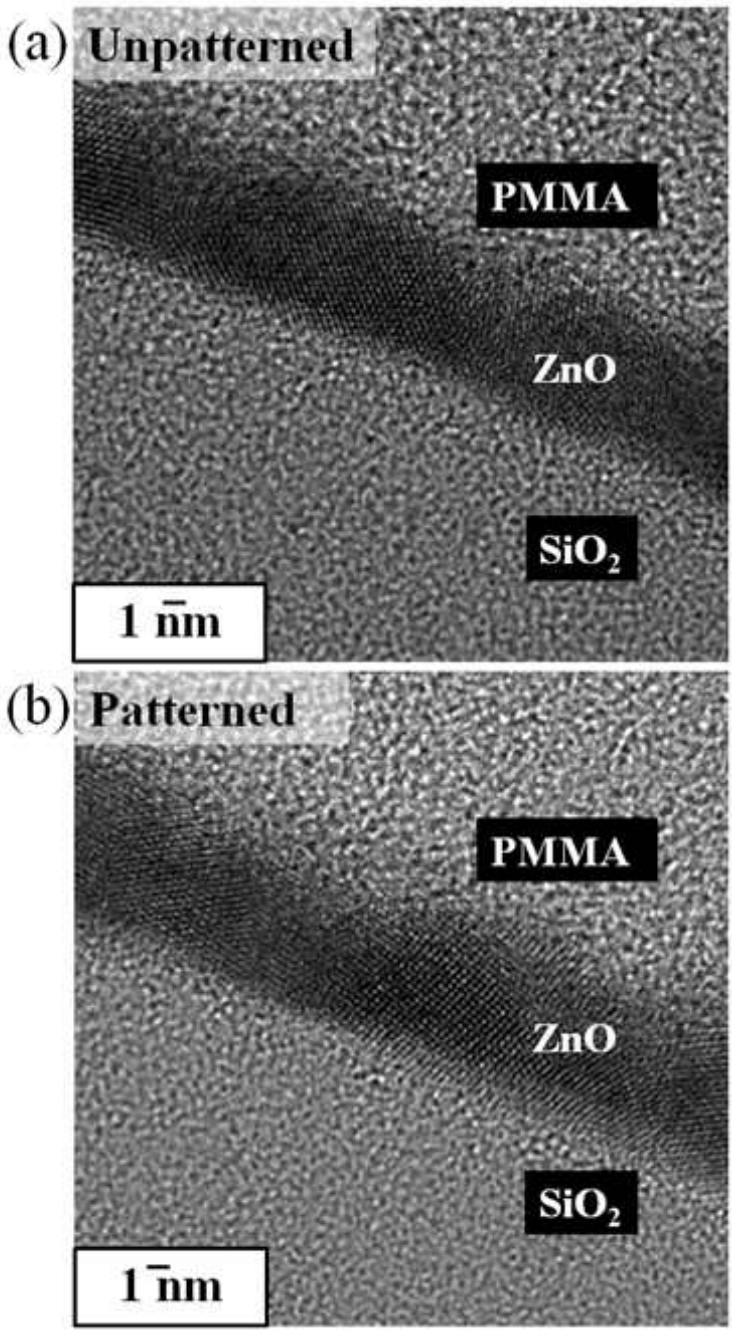

Figure 8. Transmission electron microscope images of (a) unpatterned ZnO thin films, (b) micro-patterned ZnO thin films.

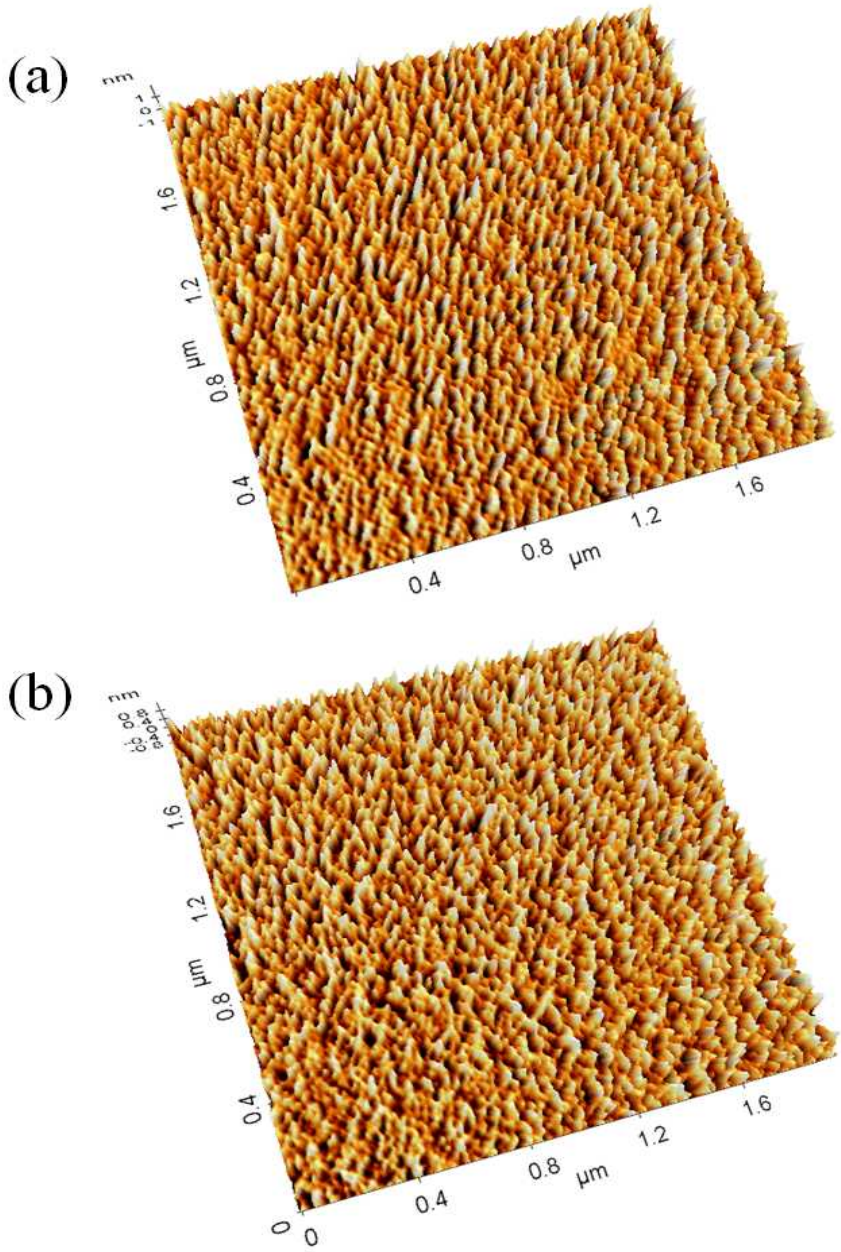

Figure 9. Atomic force microscopy images of (a) spin-coated ZnO thin films. (b) micro-patterned ZnO thin films. Root mean square roughness of spin-coated ZnO thin films were 0.324 nm; the patterned ZnO thin films were 0.222 nm.

3.4 TFT Characteristics

Figure 10 and 11 show the electrical characteristics of Li doped ZnO TFTs with a bottom gate and top contact structure. The output curves of unpatterned Li doped ZnO TFTs are shown in Figure 10 a, and the transfer curve of unpatterned Li doped ZnO TFTs are shown in Figure 11 a. The unpatterned Li doped ZnO TFTs show that the field effect mobility was 6.92 $cm^2 \cdot V^{-1} \cdot s^{-1}$, the on/off current ratio was 7.5×10^6, and threshold voltage was 12.15 V. The channel length (L) was 50 μm and the channel width of the device was 1000 μm. (W/L=20) Field effect mobility was calculated from transfer curve through Metal-Oxide Semiconductor Field Effect Transistor (MOSFET) standard model in the saturation curve, as follows.

$$I_D = \frac{W}{2L} \mu C_i (V_G - V_T)^2$$

I_D indicates the current between source and drain electrodes; W is the width of the channel; L is the length of channel between

source and drain electrodes; C_i is the capacitance of the dielectric layer (SiO_2 200 nm thickness); V_G is the voltage of gate electrode; and V_T is the saturation threshold voltage. μ is the field effect mobility that represents the characteristics of TFTs.

Figures 10 b and 11 b show the electrical characteristics of patterned Li doped ZnO TFTs by chemical imprinting. After chemical imprinting, the Li doped ZnO semiconductor patterns were fabricated as square shaped (500 μm). The process for fabrication of patterned Li doped ZnO TFTs was the same with the unpatterned Li doped ZnO TFTs via the same shadow mask on thermal evaporation of Al. The channel length (L) was 50 μm, and the channel width of the device was 500 μm (W/L=10) as the length of the semiconductor patterns. In this case, the channel length (L) was the same (50 μm) as the unpatterned TFTs; however, the channel width of patterned TFTs was shorter than unpatterned TFTs (1000 μm). The channel length and width of unpatterned TFTs were defined by electrode size as the shadow mask used in Al thermal evaporation. The geometrical channel ratio (W/L) of the un-patterned TFTs was 20, and that of patterned TFTs was 10. According to the report,

these numerical changes did not affect the field-effect mobility.[31] In Figure 10 b, the output curves represent the reasonable linear and saturation behaviors as unpatterned Li doped ZnO TFTs. The transfer curve of patterned Li doped ZnO TFTs are shown in figure 11 b. The field effect mobility was 4.2 $cm^2 \cdot V^{-1} \cdot s^{-1}$, the on/off current ratio showed 8.3×10^7, and threshold voltage was 14.05 V, as obtained from transfer curve of micro-patterned Li doped ZnO TFTs. The leakage current (10^{-9} ~ 10^{-10}A) of micro-patterned Li doped ZnO TFTs was at a considerably lower level than that of unpatterned Li doped ZnO TFTs.

The extremely low leakage current in micro-patterned Li doped ZnO TFTs was as revealed the faithful isolation of semiconductor patterns without the residual layer leading to high on/off current ratio with exclusion of off current. The hysteresis curve of micro-patterned Li doped ZnO TFTs is shown in Figure 12. As forward and reverse V_G traces, the negligible current hysteresis was observed. This curve indicated that chemical imprinting does not damage on the insulator layer. For measuring the average field effect mobility of micro-patterned Li doped ZnO TFTs, 36 points were measured from the micro-patterned Li

doped ZnO TFTs that were fabricated by one run. These numerical figures were shown in figure 13. Except for a few points, the electrical characteristics of TFTs were obtained successfully and the average field effect mobility was 4.16 $cm^2 \cdot V^{-1} \cdot s^{-1}$ on 33 points of TFTs. Although the TFTs were fabricated in the ambient condition, over 90 % of the patterned Li doped ZnO TFTs faithfully showed the electrical characteristics to exhibit uniformity.

For comparing the TFT characteristics in terms of the patterning effect, the field effect mobilities were compared from Figure 11 a and b. Unpatterned Li doped ZnO TFTs indicated 6.92 $cm^2 \cdot V^{-1} \cdot s^{-1}$; however, micro-patterned Li doped ZnO TFTs indicated 4.2 $cm^2 \cdot V^{-1} \cdot s^{-1}$ showing a slight decrease. These numerical changes do not mean that chemical imprinting might degraded the characteristics of TFTs. On the TFTs with the non-isolated semiconductor films, the fringing current exists, and this effect plays a role in overestimating the field effect mobility.[32] The fringing current is shown in figure 14 a. Therefore, the exact field effect mobility of the Li doped ZnO TFTs can be calculated excluded fringing current effect via

chemical imprinting on Li doped ZnO TFTs. The value of the field effect mobility of unpatterned Li doped ZnO TFTs seem to be somewhat exaggerated.

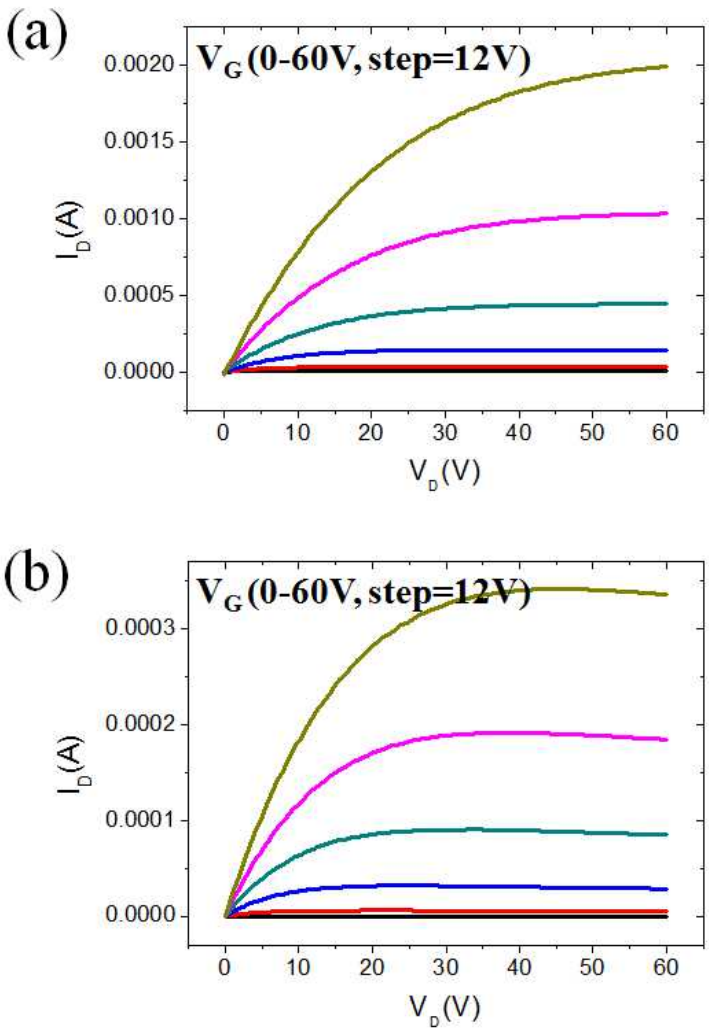

Figure 10. The output curves of (a) unpatterned Li-doped ZnO TFT, (b) the micro-patterned Li-doped ZnO TFT.

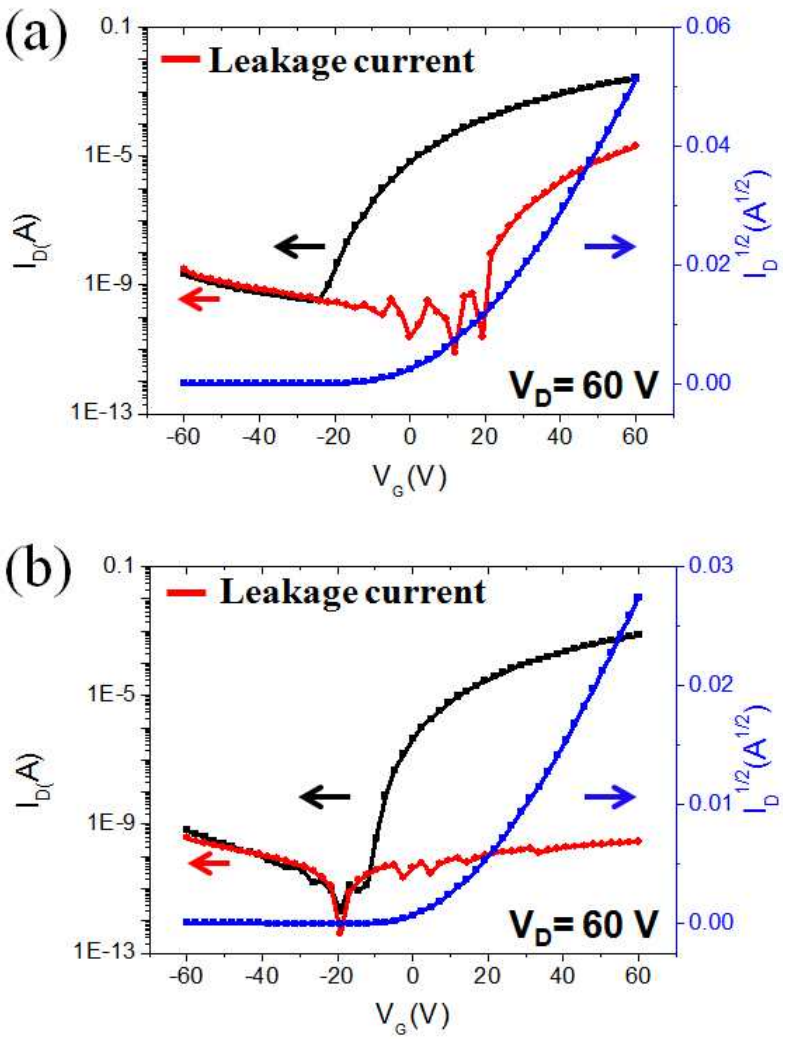

Figure 11. The transfer curves of (a) unpatterned Li-doped ZnO TFT, (b) the micro-patterned Li-doped ZnO TFT.

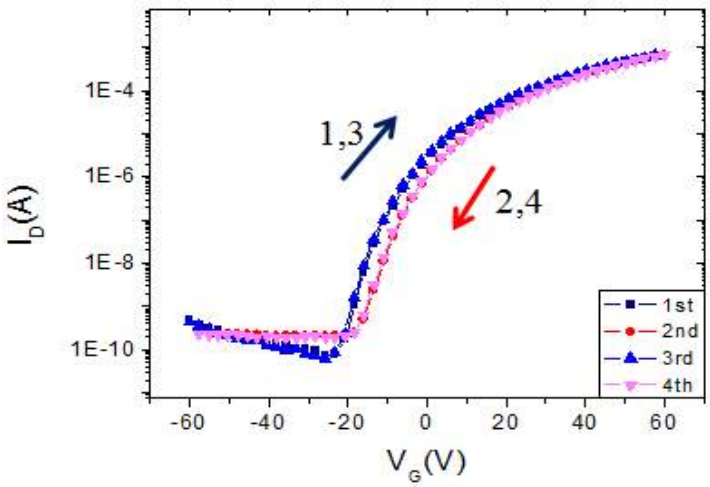

Figure 12. Hysteresis of the electrical characteristics on micro-patterned Li doped ZnO TFTs.

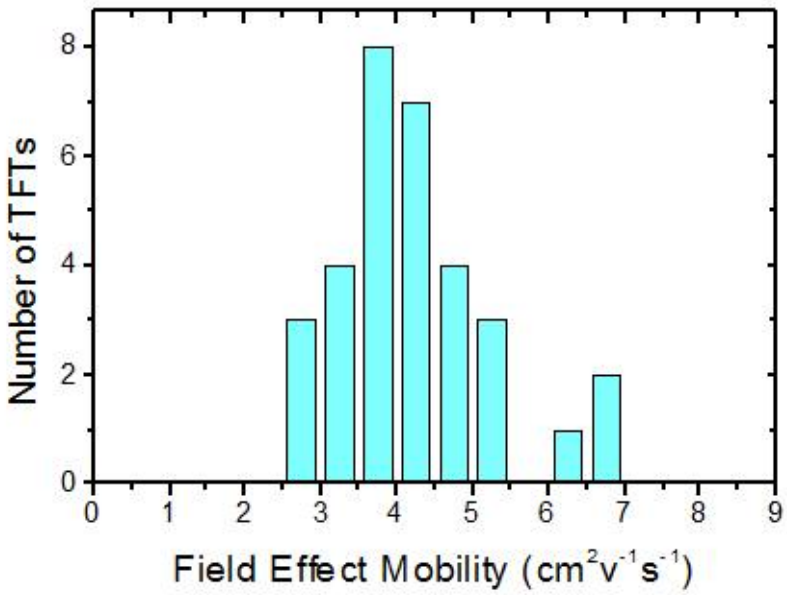

Figure 13. The field effect mobilities of micro-patterned Li doped ZnO TFTs array obtained as one-run process after sintering at 300 ℃.

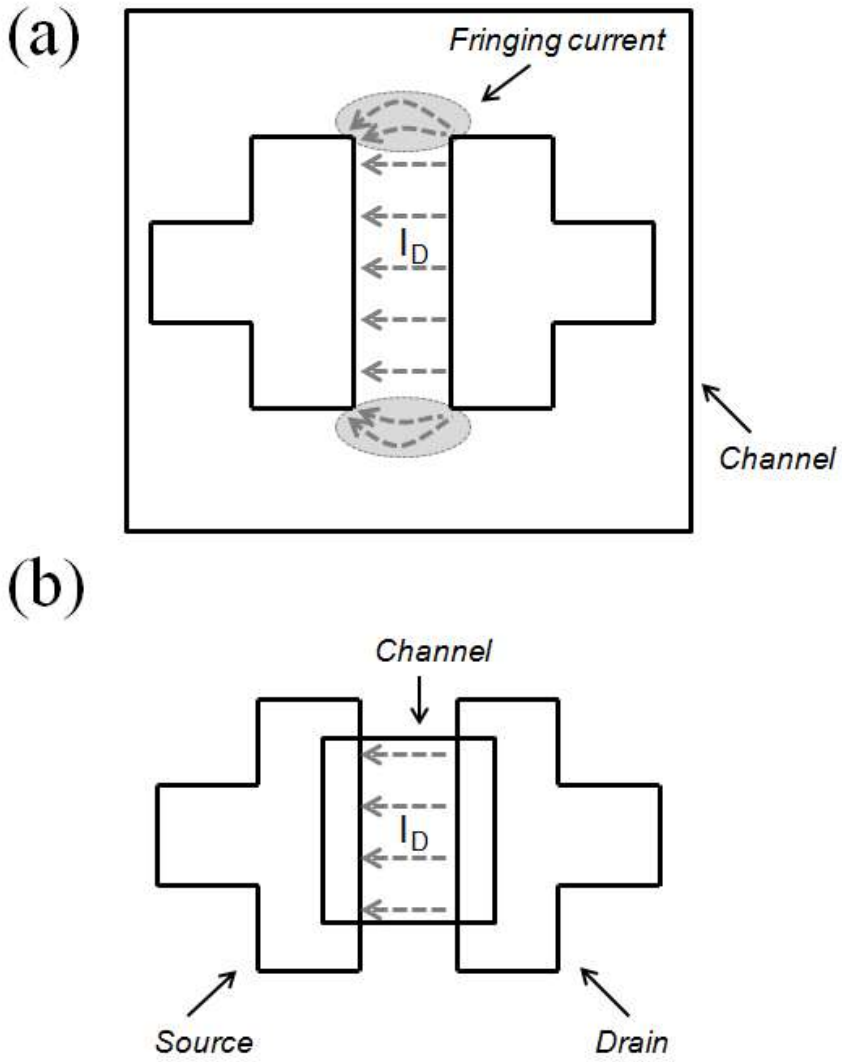

Figure 14. The schematics of current flow of (a) unpatterned device, (b) patterned device.

4. Conclusion

In conclusion, we developed a new patterning method via chemical imprinting with an ammonia soaked PDMS stamp which is simple, cost-effective, carried out in ambient conditions, and has no residual layer. Ammonia water was diffused out of the soaked PDMS stamp in a binary solvent composed of methanol and ammonia water. Diffused ammonia water formed aqueous ammine-hydroxo zinc complexes via chemical reaction on the contact regions between PDMS stamp and the ZnO thin films. These complexes were dissolved in de-ionized water due to the aqueous forms and resulted in the residual layer free micro-patterns of ZnO semiconductor films. The micro-patterned Li doped ZnO TFTs show reliable and good electrical performance without any deterioration of the interface between electrodes and semiconductor films unlike the drawbacks of the photolithography or conventional microcontact printing, as mentioned above. The representative micro-patterned Li doped ZnO TFTs indicated an average field effect mobility of 4.2

$cm^2 \cdot V^{-1} \cdot s^{-1}$ and on/off current ratio of 8.7×10^7; it considerably decreased the leakage current compared with unpatterned Li doped ZnO TFTs. We carried out the chemical imprinting via chemical reaction; thus, if the materials have a probability to react with ammonia water, this may result in the patterning process leading to the high field effect mobility of TFTs with lower off-current. This would lead to high on/off current ratio and extremely low leakage current, preventing cross-talks and signal noises. We believe that this patterning method shows a good potential for the ZnO TFTs, which indicate high field effect mobility and improvements over the printing electronic devices with metal oxide TFTs.

Reference

[1] S. H. K. Park, C. S. Hwang, M. Ryu, S. Yang, C. Byun, J. Shin, J. I. Lee, K. Lee, M. S. Oh, S. Im, Advanced Materials **2009,** *21,* 678-682.

[2] J. Y. Kwon, D. J. Lee, K. B. Kim, Electronic Materials Letters **2011,** *7,* 1-11.

[3] J. S. Park, W. J. Maeng, H. S. Kim, J. S. Park, Thin Solid Films **2012,** *520,* 1679-1693.

[4] T. Kamiya, K. Nomura, H. Hosono, Journal of Display Technology **2009,** *5,* 273-288.

[5] A. Nathan, A. Ahnood, M. T. Cole, S. Lee, Y. Suzuki, P. Hiralal, F. Bonaccorso, T. Hasan, L.Garcia-Gancedo, A. Dyadyusha, S. Haque, P. Andrew, S. Hofmann, J. Moultrie, D. Chu, A. J. Flewitt, A. C. Ferrari, M. J. Kelly, J. Robertson, G. A. J. Amaratunga, and W. I. Milne, Proceedings of the IEEE **2012,** *100,* 1486-1517

[6] K. Nomura, H. Ohta, A. Takagi, T. Kamiya, M. Hirano, H. Hosono, Nature **2004,** *432,* 488-492.

[7] T. Kamiya, H. Hosono, Npg Asia Materials **2010,** *2,* 15-22.

[8] S. Masuda, K. Kitamura, Y. Okumura, S. Miyatake, H. Tabata, T. Kawai, Journal of Applied Physics **2003,** *93,* 1624-1630.

[9] P. F. Carcia, R. S. McLean, M. H. Reilly, G. Nunes, Applied Physics Letters **2003,** *82,* 1117-1119.

[10] J. Jo, O. Seo, H. Choi, B. Lee, Applied Physics Express **2008,** *1,* 041202.

[11] S. J. Lim, S. J. Kwon, H. Kim, J. S. Park, Applied Physics Letters **2007,** *91,* 183517.

[12] Chnnupati Jagadish and Stephene J. Pearton, *Zinc oxide Bulk, Thin Films and Nanostructures: Processing, Properties, and Applications.* (Elsevier, 2006, 415-421)

[13] G. M. Wallraff, W. D. Hinsberg, Chemical Reviews, **1999,** *99,* 1801-1821.

[14] K. Kim, S. Park, J. B. Seon, K. H. Lim, K. Char, K. Shin, Y. S. Kim, Advanced Functional Materials **2011,** *21,* 3546-3553.

[15] C. Punset, J. P. Boeuf, L. C. Pitchford, Journal of Applied Physics **1998,** *83,* 1884-1897

[16] S. H. K. Park, C. S. Hwang, H. Y. Jeong, H. Y. Chu, K. I.

Cho, Electrochemical Solid States **2008,** *11,* H10-H14.

[17] S. H. K. Park, D. H. Cho, C. S. Hwang, S. Yang, M. K. Ryu, C. W. Byun, S. M. Yoon, W. S. Cheong, K. I. Cho, J. H. Jeon, ETRI Journal. **2009,** *31,* 653-659.

[18] M. Kim, J. H. Jeong, H. J. Lee, T. K. Ahn, H. S. Shin, J. S. Park, J. K. Jeong, Y. G. Mo, H. D. Kim, Appl.ied Physics Letters **2007,** *90,* 212114.

[19] G. H. Kim, H. S. Kim, H. S. Shin, B. D. Ahn, K. H. Kim, H. J. Kim, Thin Solid Films **2009,** *517,* 4007-4010.

[20] D. Kim, Y. Jeong, C. Y. Koo, K. Song, J. Moon, Japanese Journal of Applied Physics **2010,** *49,* 05EB06.

[21] T. L. Breen, P. M. Fryer, R. W. Nunes, M. E. Rothwell, Langmuir **2002,** *18,* 194-197.

[22] S. T. Meyers, J. T. Anderson, C. M. Hung, J. Thompson, J. F. Wager, D. A. Keszler, Journal of the American Chemical Society **2008,** *130,* 17603-17609.

[23] Y.-H. Kim, J.-S. Heo, T.-H. Kim, S. Park, M.-H. Yoon, J. Kim, M. S. Oh, G.-R. Yi, Y.-Y. Noh and S. K. Park, Nature **2012,** *489,* 128-132

[24] E. M. C. Fortunato, L. M. N. Pereira, P. M. C. Barquinha, A.

M. B. do Rego, G. Goncalves, A. Vila, J. R. Morante, R. F. P. Martins, Applied Physics Letters **2008,** *92,* 222103.

[25] S. Y. Park, B. J. Kim, K. Kim, M. S. Kang, K. H. Lim, T. Il Lee, J. M. Myoung, H. K. Baik, J. H. Cho, Y. S. Kim, Advanced Materials **2012,** *24,* 834-838.

[26] C.H. Park, S.B.Zhang, S. H. Wei, Physical Review B. **2002,** *66,* 073202

[27] S. B. Orlinskii, J. Schmidt, P. G. Baranov, D. M. Hofmann, C. D. Donega, A.Meijerink, Physical Review Letters **2004,** *92,* 047603

[28] J. J. Richardson, F. F. Lange, Crystal Growth & Design **2009,** *9,* 2570-2575.

[29] J. N. Lee, C. Park, G. M. Whitesides, Analytic Chemistry **2003,** *75,* 6544-6554.

[30] Y. N. Xia, G. M. Whitesides, Angewandte Chemistry International Edition **1998,** *37,* 551.

[31] K. Okamura, D. Nikolova, N. Mechau, H. Hahn, Applied. Physics Letters **2009,** *94,* 183503.

[32] J. H. Jeon, Y. H. Hwang, B. S. Bae, Electrochemical Solid States **2012,** *15,* H123-H125

요 약 (국문초록)

암모니아를 흡수시킨 PDMS 스탬프를 이용하여 산화아연 전구체 용액을 스핀코팅하여 형성한 박막에 화학적인 임프린팅 공정을 이용하여 패터닝 공정을 진행하였다. 산화아연은 암모니아와 반응을 하여 수용성 염을 형성하기 때문에 암모니아를 흡수시킨 PDMS 스탬프로부터 암모니아가 빠져나와 산화아연 박막과 접촉된 부분에서 선택적으로 수용성 염인 $[Zn(NH_3)_{4-n}(OH)_n]^{2-n}$ 형태로 변환시킨다. 이 선택적으로 변환된 염은 물에 녹일 수 있다. 이렇게 형성된 마이크로 사이즈의 산화아연 패턴은 박막 트랜지스터의 반도체 층에 적용될 수 있다. 그래서 실리콘 옥사이드 200 nm를 가진 실리콘 웨이퍼 위에 리튬을 도핑한 산화아연 박막을 형성한 뒤, 화학적인 임프린팅 공정을 이용하여 마이크로패턴을 형성하였다. 산화아연 박막의 소결 온도는 300 °C였다. 이 마이크로 패턴 위에 열증착과정을 통해 알루미늄을 소스/드레인 전극으로 증착하여 박막트랜지스터를 형성한 뒤 소자의 성능을 관찰하였다. 대표 소자의 전계 효과 전자 이동도는 4.2 $cm^2 \cdot V^{-1} \cdot s^{-1}$, on/off 전류비는 8.3 x 10^7를 나타냈으며 패터닝 공정을 진행하지 않은 소자에 비해 낮은 누설전류 값을 나타내어 패터닝 공정이 잘 진행되었음을 확인할 수 있었다. 이 화학적인 임

프린팅 공정은 용액 공정으로 형성된 산화아연 박막에 대해 적합하다. 또한 이 공정은 대기 중에서 연속적인 공정인 롤투롤 공정에 이용 가능하며 포토리소그래피처럼 번거로운 공정 단계들이 요구되지 않는 간단한 공정법이다.

주요어 : 임프린트 리소그래피, 소프트 리소그래피,
산화아연 반도체, 박막트랜지스터, 화학적 에칭

학 번 : 2011-22754